

A 90°-Bent Spur-Line Combined CRLH ZOR Bandpass Filter for the Channel of the UWB Communication System

Changhyeong Lee* and Sungtek Kahng†

Abstract – In this paper, a compact fully printable bandpass filter is suggested for a low-frequency channel 3.2 GHz ~ 3.7 GHz in the Ultra-Wideband (UWB) communication system. It is featured with a small geometry of $0.5\lambda_g/15$ and a low insertion loss despite using FR4 as a cheap substrate of a high dielectric loss. This is made possible by generating zeroth-order-resonance (ZOR) from one cell comprising two series resonances obviously separated from one shunt resonance as a third-order bandpass filter. Especially, the series resonance elements are combined with spur-lines bent by 90 degrees, which makes the port-impedance matched well and eliminates spurious hikes in the stopband, while the overall size remains almost unchanged. The design is carried out by setting up the equivalent circuit and the circuit simulation is checked by the full-wave EM analysis. The structure is manufactured and measured to show that the circuit modeling and EM simulation results agree with the measured data.

Keywords: Metamaterial, CRLH transmission line, ZOR, Bandpass filter

1. Introduction

The UWB communication is adopted by low-power pulse transmission and thru-wall imaging technologies. Also, the UWB lower-half band (3.1 GHz~4.8 GHz) is discussed for the WVAN and Home Networking field [1]. The quality of the communication is heavily dependent on the successful implementation of the RF components, and the system developers have been driven to meet the demand of small sizes, light weight, low interference, low power consumption, etc. To reduce the overall size of a UWB system, the key passive components such as filters should be as compact as can be, and extensive work has been reported to design UWB BPFs, e.g., stub and lumped element loading, composite low pass-high pass topology, cascaded broadside-coupling and multiple-mode resonator (MMR) [2,3]. These methods still face the restrictions on miniaturization and low insertion loss (low power consumption).

In order to improve filter designs, a number of techniques have been exploited. Allison modified the configuration of the parallel-edge coupled filter into multiple coupled resonators to make it smaller than other parallel-edge coupled filters [4]. Yu and Chang employed the open-loop resonators coupled with crossing lines to reduce the filter size and to have an elliptic function response [5]. These filters have half guided-wavelength resonators. As an alternative approach for enhanced size-reduction, stepped

impedance resonators are embedded in the open-loops by J. Zhang et al [6]. However, it undergoes an unwanted capacitive coupling between stepped impedance resonators.

Lately, the metamaterial (MTM) area was introduced and it shows intriguing phenomena called Zeroth Order Resonance (ZOR) and Negative Resonance (NR), when designed correctly. C. Caloz et al presented a periodic multi-celled Composite Right/Left-handed (CRLH) transmission line with NR, ZOR, and Positive Resonance [7]. At the ZOR, the fields have no-phase variation over the transmission line. R. Marques et al used the periodic structure with a finite number of multi cells composed of a rectangular patch with a shorting pin or a strip beside SRRs to form stopbands or passbands [8]. These structures are periodic by replicating a size and a shape. On the other hand, non-periodic metamaterial filters were devised with ZOR characteristics as a single-stage structure [9-11].

In this paper, a new design method is proposed for making fully printable and miniature bandpass filter for channel 3.2 GHz~3.7 GHz. To make this passband as a small ZOR structure of the third-order filtering, two series resonators are connected through one shunt resonator. For impedance match at input and output ports, spur-lines are bent at a right angle and used to combine the input port and the central mushroom as the shunt resonator. This applies to the central mushroom and the output port. The proposed method enhances insertion loss and size-reduction properties from half-wavelength resonator-based techniques and definitely differs from other ZOR filters in that the proposed scheme picks up C_L and L_R from the CRLH-line to make the series and singles C_R and L_L out to compose the shunt resonator, while others do not. This approach enables us to determine the filter order exactly and the

† Corresponding Author: Dept. of Information & Telecommunication Engineering, Incheon National University, Incheon, Korea. (s-kahng@inu.ac.kr)

* Dept. of Information & Telecommunication Engineering, Incheon National University, Incheon, Korea. (Antman@inu.ac.kr)

Received: May 15, 2017; Accepted: December 29, 2017

overall size to be as small as $0.5\lambda_g/15$ and filter to meet the passband with the third-order filtering. The method includes the circuit modeling resulting in agreement with the full-wave EM simulation. Besides, the small difference between the EM simulation and measurement results validates the proposed method. Additionally, the CRLH ZOR properties are verified with the E-field distributions over the geometry, and dispersion diagrams.

2. Equivalent Circuit for the CRLH ZOR Bandpass Filter

Prior to the main part of the design, the specification of the channel filter can be seen in the Table 1.

Table 1. The specification of the channel filter

Spec. Items	Figure	Note
Band	3.2 GHz~3.7GHz	Bandwidth : 500 MHz
Insertion Loss	< 1.5 dB	Consideration : relative permittivity of substrate
Return Loss	< -15 dB	In the passband
Isolation (Skirt)	> 14 dB @Cutoff $\pm \approx 30$ MHz	

The schematic of the CRLH transmission line is depicted in Fig. 1. The left-handed part of Fig. 1 as a metamaterial has been examined theoretically and experimentally as it holds the duality about the right-handed part, and its unit cell has the series inductance and shunt capacitance and series capacitance and shunt inductance all together, whose size is smaller than the guided wavelength, when they satisfy the conditions of the zero or negative phase constant [7, 9-11]. Therefore, the CRLH TL has no phase variation with the ZOR, phase advance with the left-handedness, and phase delay with the right-handedness. The basic design equations for the CRLH TL are the resonance frequencies of the left-handedness, right-handedness, and series and shunt resonators from Fig. 1 as follows:

$$\omega_L = \frac{1}{\sqrt{L_L C_L}}, \quad \omega_R = \frac{1}{\sqrt{L_R C_R}} \quad (1)$$

$$\omega_{se} = \frac{1}{\sqrt{L_R C_L}}, \quad \omega_{sh} = \frac{1}{\sqrt{L_L C_R}}, \quad \omega_0 = \sqrt{\omega_L \omega_R} \quad (2)$$

where ω_L , ω_R , ω_{se} , ω_{sh} , and ω_0 mean the resonance frequencies of the left-handed part, right-handed part, series resonator, shunt resonator of Fig. 2, and the center frequency, respectively, for channel 3.2 GHz ~ 3.7 GHz.

The asymmetric type CRLH equivalent circuit in Fig. 1(a) changes to the T type in Fig. 1(b) for the ease in physically implementing the coupling elements between the resonators to create a passband of the filter. This passband will be formed as the zone from the LH region through the ZOR point to the RH region, which will be

shown later with the dispersion diagram as the relation between the frequency and the propagation constant (β_0) in the balanced condition similar to [7, 9-11]. The basic formulas are

$$Z_L = \sqrt{\frac{L_L}{C_L}}, \quad Z_R = \sqrt{\frac{L_R}{C_R}} \quad (3)$$

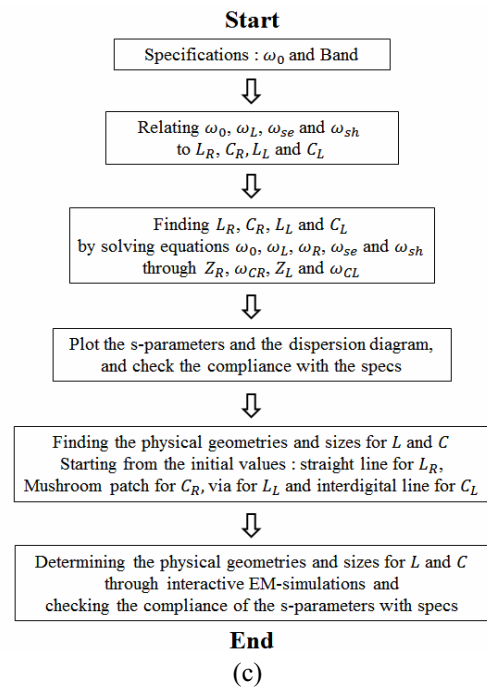
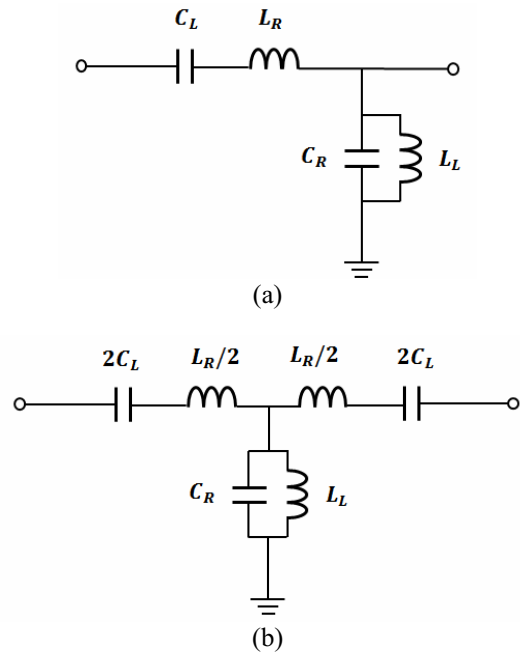


Fig. 1. The CRLH Transmission line equivalent BPF circuit and design procedures (a) Asymmetric type equivalent circuit (b) T-type equivalent circuit (c) Design steps

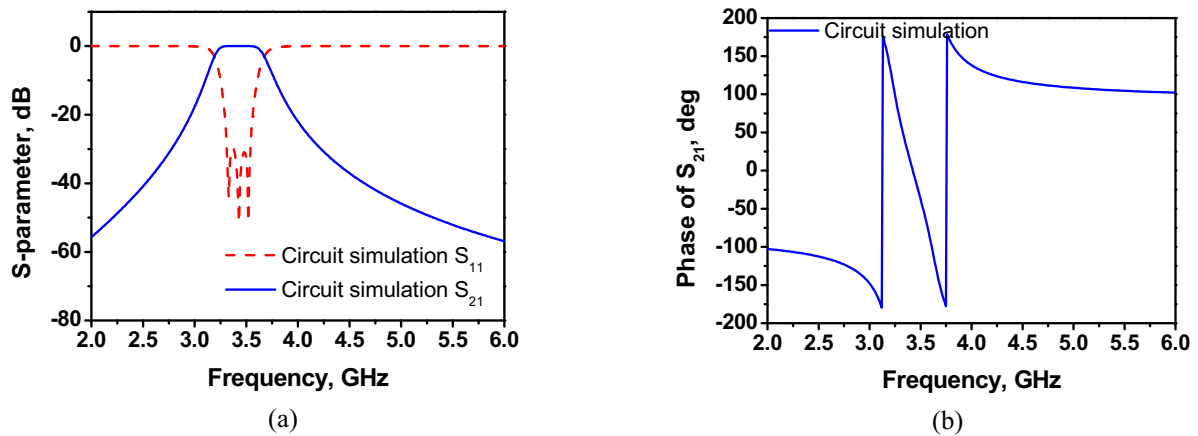


Fig. 2. Properties of the equivalent circuit of the CRLH ZOR bandpass filter (a) Magnitudes of S_{11} and S_{21} of the filter for the channel (b) Phase of S_{21} from the filter

$$\omega_{cL} = \omega_R \left| 1 - \sqrt{1 + \frac{\omega_L}{\omega_R}} \right|, \quad \omega_{cR} = \omega_R \left| 1 + \sqrt{1 + \frac{\omega_L}{\omega_R}} \right| \quad (4)$$

In the balanced condition, the RH impedance Z_R and the LH impedance Z_L are equal to characteristic impedance Z_0 . And the band of the filter is determined by $\omega_{cL} (= 2\pi f_{cL})$ and $\omega_{cR} (= 2\pi f_{cR})$ [9-11].

$$C_R = \frac{2}{Z_R(\omega_{cR} - \omega_{cL})} \quad (5)$$

$$L_R = Z_R^2 C_R \quad (6)$$

$$C_L = \frac{C_R}{\left(\left(\left(\frac{(\omega_{cR} + \omega_{cL}) Z_R Z_L}{2} \right)^2 - 1 \right) \right)} \quad (7)$$

$$L_L = Z_L^2 C_L \quad (8)$$

By equating f_{cL} and f_{cR} to 3.2 GHz and 3.7 GHz, with the ZOR at ω_0 , the CRLH circuit parameters are calculated as Table 2.

Table 2. Circuit parameters of the CRLH ZOR bandpass filter for the channel

Band (f_{cL} and f_{cR})	L_L [nH]	L_R [nH]	C_L [pF]	C_R [pF]	Z_0 [ohm]
3.2 GHz ~ 3.7 GHz	0.168	31.831	0.067	12.732	50

With L_L , L_R , C_L , and C_R above for the characteristic impedance $Z_0 = 50\Omega$, we investigate the impedance matching and accompanying properties through the circuit simulation, and the magnitude and phase of the frequency response that are plotted in Fig. 2.

Fig. 2(a) presents the magnitude of the s-parameters as the frequency responses of the equivalent circuit of the channel. S_{21} shows the passband 3.2 GHz ~ 3.7 GHz as the channel, and S_{11} is lower than -15 dB in the passband

where three poles due to two series resonances and one shunt resonance. Also, the poles in S_{11} correspond to the frequencies where the phase of S_{21} becomes zero degree and $\pm 180^\circ$ as in Fig. 2(b). The phase response of Fig. 2(b) has zero β_0 at the center frequency (3.45 GHz for the channel).

3. Realizing the CRLH ZOR Bandpass Filter

The physical dimensions of the filter will be found to realize the calculated equivalent circuit parameters. So the physical geometry for the filter is simulated with a 3D EM analysis program and the substrate for the microstrip structure is treated as the FR-4 with the dielectric constant 4.4, height of substrate 1 mm, and loss tangent 0.02. As the proposed ZOR filter consists of two series resonators and one shunt resonator, individual resonators are realized one after another. Firstly, we deal with the series resonator which is the combination of interdigital coupled lines and a straight thin line as shown in Fig. 3(a). The interdigital coupled lines are chosen for C_L , and their approximate relationship is mentioned [9-11]. The straight thin line accounts for is L_R and its physical dimensions Wl and Ll are evaluated as in [9-11]. The spur-lines as the interdigital coupled lines and the straight line segment are put together in the full-wave simulator and changed bit by bit and finalized when the EM simulation has good agreement with the circuit simulation as presented in Fig. 3.

The inductance of the series resonator is found from the curve of the extracted L and the dumbbell-shaped spur-line structure in the EM simulator as in Fig. 3(b). The series capacitance of the series resonator is realized by the relationship in Fig. 3(c). Dependent on the number of interdigital-line fingers, different C is made. Since this is not a complete filter but a resonator, it is checked if the target resonance frequency is achieved. These procedures are not shown in other papers. As shown in the magnitude and phase of s-parameters in Fig. 3(d) and (e), the series

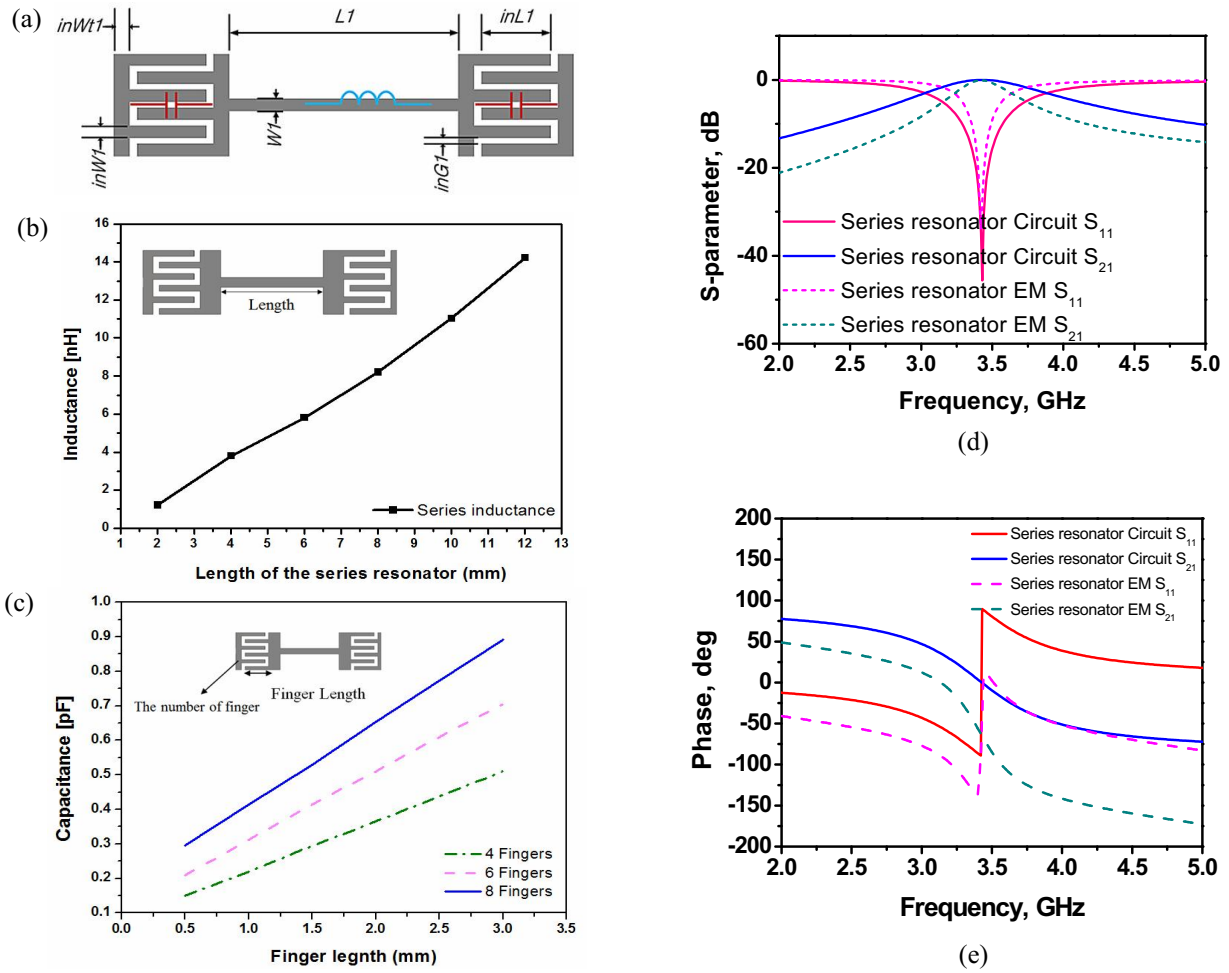


Fig. 3. The series resonator of the CRLH BPF for the channel: $inWt1 = 0.1$ mm, $inL1 = 1.7$ mm, $inG1 = 0.1$ mm, $inWt1 = 1.4$ mm, $w1 = 0.4$ mm, and $L1 = 7.7$ mm (a) Physical geometry (b) L in the circuit and the spur-line dumbbell's length (c) C in the circuit and the spur-line finger length and number of the fingers (d) Comparison of the frequency responses between the circuit and EM simulations (e) Comparison of the phases of the circuit and EM simulations

resonator is designed correctly to have the center frequency 3.45 GHz where the insertion loss is 0 dB and the return loss is less than -15 dB. This straight line-shape element is modified to bent spur-lines in a later section.

Next, the shunt resonator of the proposed bandpass filter is dealt with about its physical shape and dimensions. The mushroom structure is adopted for the shunt resonator as shown in Fig. 4(a). The patch and the ground make capacitance C_R , and the shorted via becomes shunt inductance L_L of the shunt resonator for the ZOR BPF.

The calculated shunt L is realized by the curve extracted from EM analysis of the via height as in Fig. 4(b). The target shunt C is obtained using the curve from EM simulation of the mushroom width. These steps are not found in other literatures. As a shunt resonator, the target resonance frequency is achieved as plotted in Fig. 4(b) and (c) to have the center frequency 3.45 GHz with the sharp phase change where the insertion loss is 0 dB and the return loss is less than -15 dB.

To meet the specification of the proposed filter we have

combined two series resonators and one shunt resonator to implement a 3rd order CRLH ZOR filter. The conceptual diagram can be seen in the Fig. 5(a). The actual physical structure is shown in Fig. 5(b). However, the proposed structure increases the size of the whole structure because the series resonator is quite long to use the real estate. So, to reduce size of the CRLH ZOR filter, we proposed the structure which is the series resonator is bent spur-lines by 90° as shown in Fig 6(a). The original shapes and sizes are changed from those in designing individual series and shunt resonators, which is inevitable in physically assembling the pieces and meeting the specifications on the electrical performances. Particularly, the straight thin lines adjusted and suitable for large L_R in the proposed bandpass filter are longer and thinner than the connecting line segments in the conventional CRLH unit-cells, which leads one dumbbell-type interdigital line structure to two finger blocks facing opposite directions as 90° -bent spur-lines and attached to the ends of a thin line perpendicular to the finger blocks. Besides, our mushroom is different from the

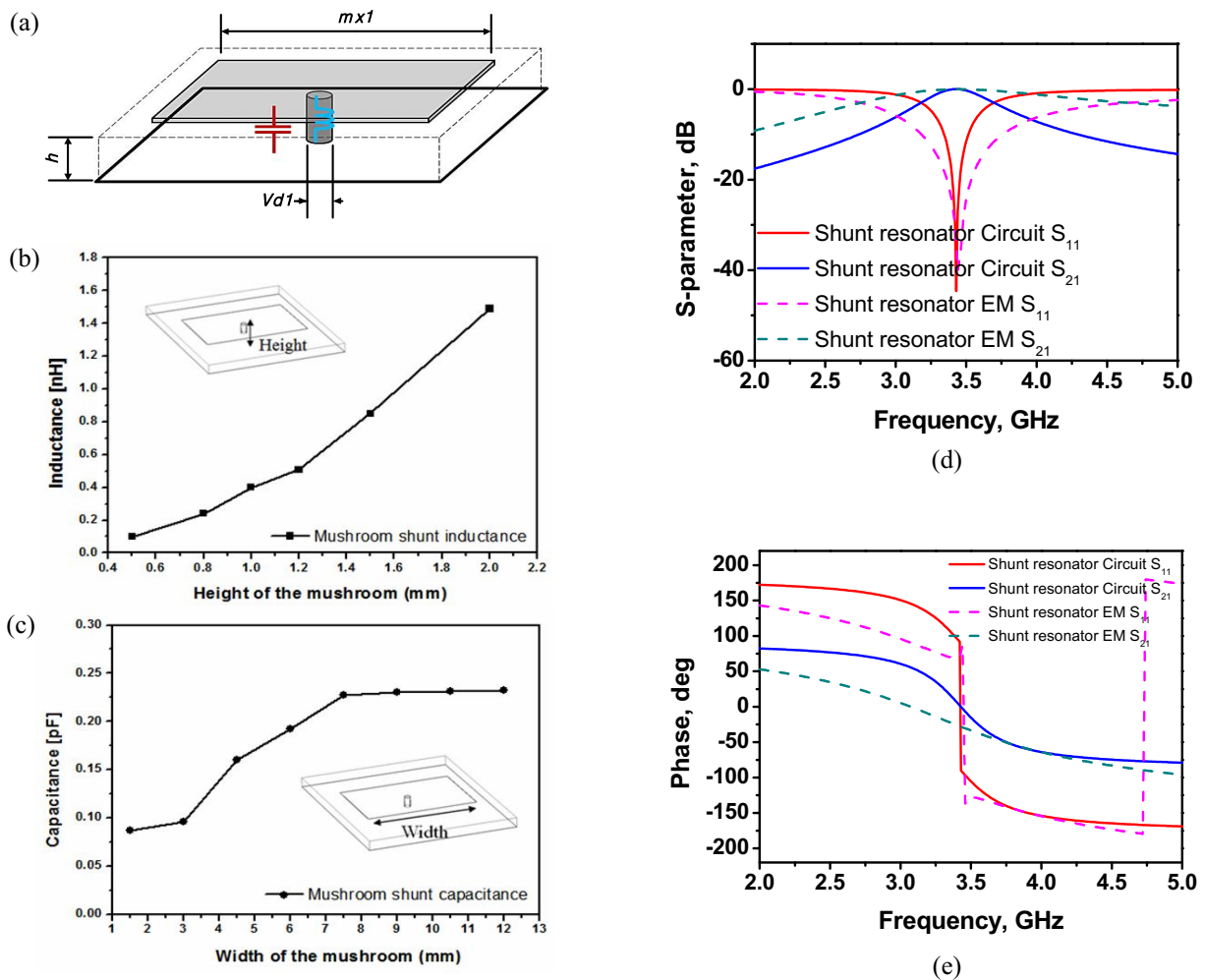


Fig. 4. The shunt resonator of the CRLH BPF for channel1: $mx1 = 9\text{mm}$, $h = 1\text{mm}$, and $Vd1 = 1.2\text{mm}$ (a) Physical geometry (b) L in the circuit and the mushroom height (c) C in the circuit and the mushroom width (d) Comparison of the frequency responses between the circuit and EM simulation (e) Comparison of the phases of the circuit and EM simulation

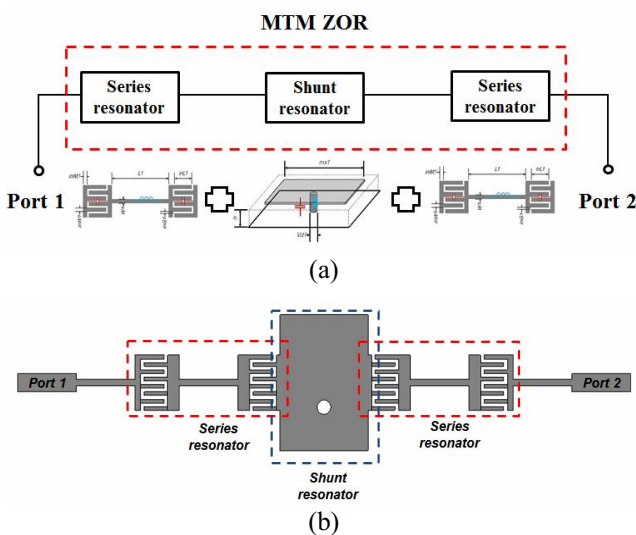


Fig. 5. The combination design of the two series resonator and one shunt resonator (a) Block diagram (b) Physical geometry

previous one to have the offsets of the via and fingers from the center of the patch.

The frequency response of the filter structure in Fig. 6(a) is calculated by the full-wave analysis simulator and is given in Fig. 6(b) and (c) with the passband where the insertion loss is nearly 0 dB, the return loss is less than -15 dB, and the phase changes between -180° and 180° . They agree well with circuit simulated results except that the full-wave simulation has the slightly increased bandwidth, which may be caused by decreased parasitic of the physical geometry for L_R and C_R , but is not significant for the relationship between the channels.

Besides the characteristics of the filter performance, we investigate the no-phase variation at the ZOR point and the LH below the ZOR.

Fig. 7(a) shows the electric field vectors that have the same direction over the entire geometry as the ZOR. Fig. 7(b) presents the backward wave of the LH region below the ZOR point as the wave front departs at port 2 at the early time (phase 20°) and wave front arrives at port 1 at

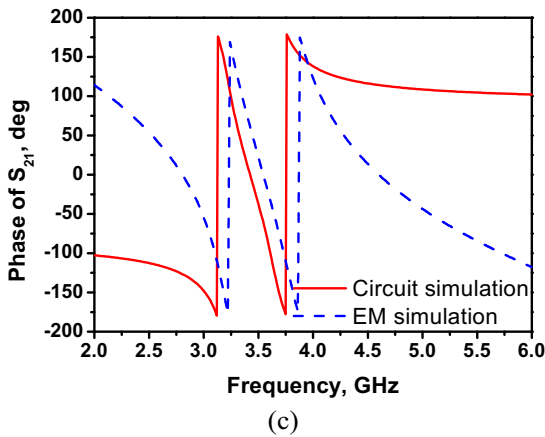
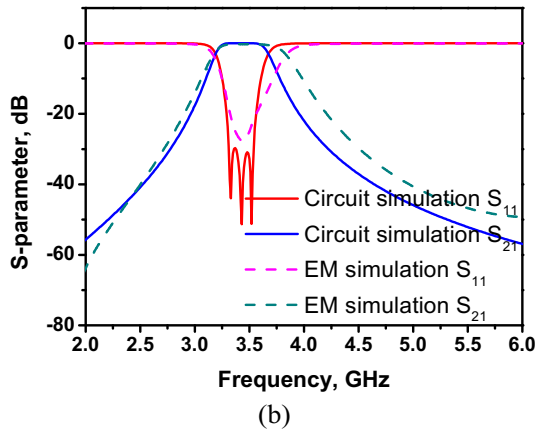
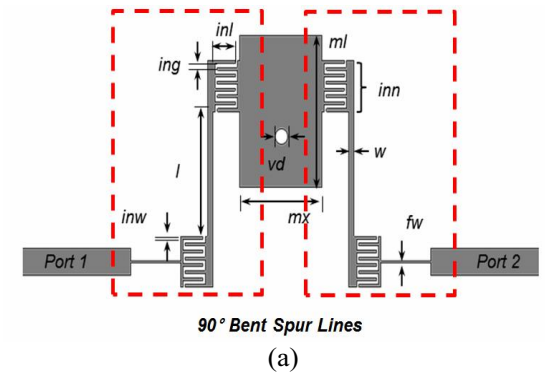


Fig. 6. Proposed CRLH ZOR bandpass filter for the channel: $inl=1.6$ mm, $ing=0.2$ mm, $inw=0.2$ mm, $w=0.5$ mm, $l=9.1$ mm, $mx=7.4$ mm, $ml=11.1$ mm, $vd=1$ mm, $fw=0.1$ mm (a) Physical geometry (b) Comparison of the frequency responses between the circuit and EM simulation (c) Comparison of the phases of the circuit and EM simulation

the late time (phase 340°). This proves the CRLH properties of the proposed design and it is predicted that the effective size-reduction is possible by the proposed method, free from the resonance condition of half-wavelength. As a conventional filter, a parallel-edge coupled type is frequently used, and is compared with the proposed filter in terms of the size and frequency response as follows.

With regard to the same order filtering, the size of the

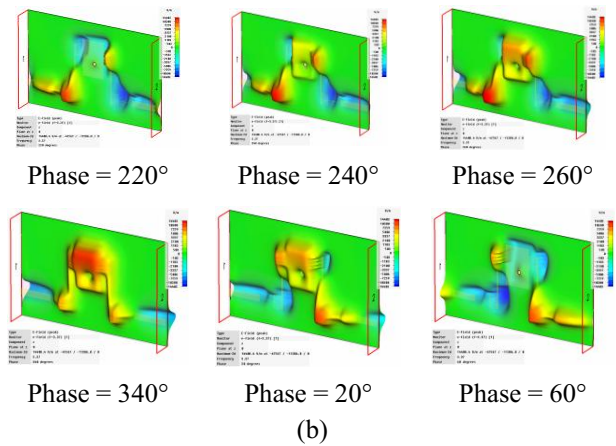
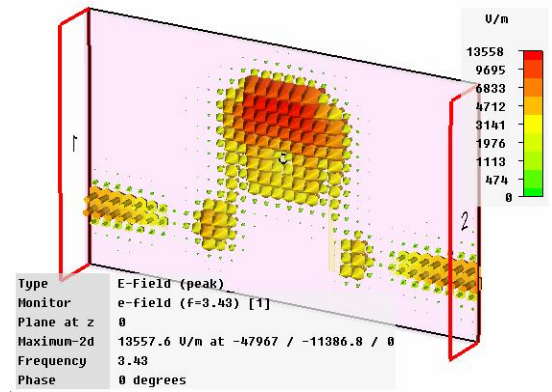


Fig. 7. E-field distributions at the ZOR and in the LH region (a) E-field distribution at ZOR (3.43 GHz) (b) E-field distribution below the ZOR point (3.3 GHz)

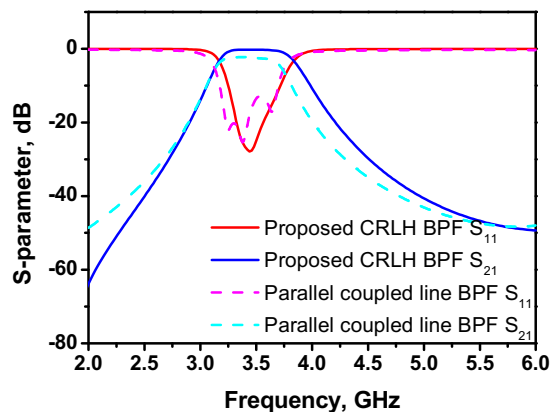


Fig. 8. Comparing the proposed compact bandpass filter with the parallel-edge coupled type of the conventional techniques

proposed bandpass filter is 2.8 times smaller than conventional bandpass filter as shown in Fig. 8 as 60%-miniaturization where our filter has the insertion loss remaining nearly 0 dB and return loss less than -15 dB in the passband. Comparing the proposed structure to the

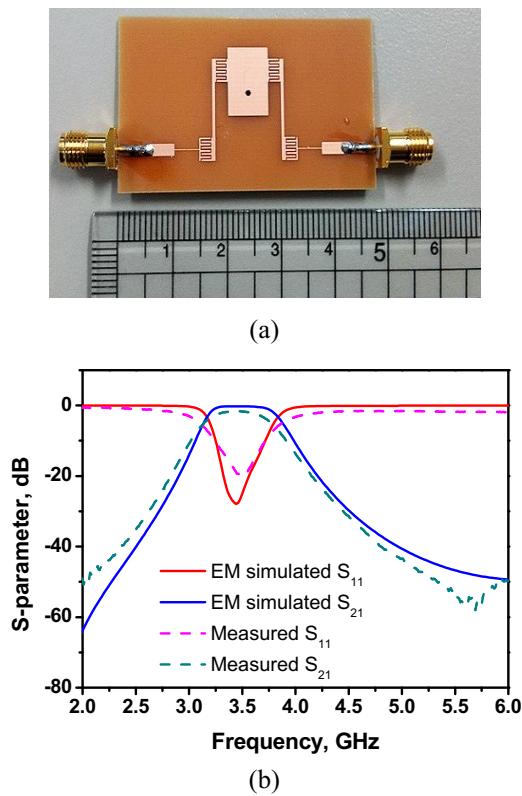


Fig. 9. Fabricated proposed CRLH bandpass filter for the channel (a) Photo of the fabricated CRLH bandpass filter (b) Comparing the simulated and measured results

conventional structure, we obtained a smaller size and lower insertion loss. They are 0.2 dB and 1 dB respectively. It also has very flat characteristics in the passband with a less than 50% amplitude deviation. To verify the design method suggested in this paper using the circuit and EM simulations, the bandpass filter for the channel is fabricated and its frequency responses are measured.

Fig. 9(a) is the photo of the fabricated CRLH bandpass filter that has the FR-4 substrate. When the the simulated and measured results are compared as in Fig. 9(b), they are in good agreement in terms of the bandwidth with the insertion loss remaining nearly 0 dB (≈ 0.7 dB) and return loss less than -15 dB in the passband and the band is achieved for the channel. With regard to the stopband, the sharpness of the curve is observed with 7dB and 22 dB attenuation at 0.5 GHz and 0.55 GHz offset from the center frequency, respectively. Moreover, due to the spur-line, the harmonic is not generated up to double the center frequency. Especially, it should be noted that while FR-4 is an unwelcome material due to relatively high loss, this design scheme could provide excellence in the loss performances.

In the Table 3, the proposed filter is compared with the previously reported filters, where λ_g denotes guided wavelength at the center frequency. The proposed filter outperforms all other configurations. Simultaneously, it has

Table 3. Differences between the proposed and previous works

Ref.	Freq. (GHz)	RL (dB)	IL (dB)	Size (λ_g @ Center freq.)
[12]	2.3-3.7	< -12	1	$\lambda_g \times 0.9\lambda_g$
[13]	1.77-1.83	< -15	3.5	$0.67\lambda_g \times 0.36\lambda_g$
[14]	1.75-2.15	< -10	11.7	$3.1\lambda_g \times \lambda_g$
[15]	2.15-2.25	< -10	<3.5	$0.25\lambda_g \times 0.38\lambda_g$
[16]	2.95-3.25	< -15	2.8	$0.66\lambda_g \times 0.2\lambda_g$
[17]	3.77-4.17	< -10	2.1	$0.4\lambda_g \times 0.11\lambda_g$
This work	3.2-3.7	< -15	1.8	$0.59\lambda_g \times 0.59\lambda_g$

a small size and good in-band characteristic. Especially, compared with the filters fabricated by the conventional method [12-14], the size difference is created due to the characteristic of the ZOR, because it is possible to generate a resonance regardless of the size. In addition, the size of the proposed filter resonator is smaller than that other designs of the CRLH concept filters [15-17] and insertion loss is also better with in the same technology. Simply speaking, the proposed design results in a lower insertion loss for FR4, while the others use relatively expensive substrates. Also, this work provides the proof of the CRLH ZOR effect. This enables the design results to be improved from those of the other techniques as seen in the comparison table above and [18].

4. Conclusion

In this paper, a new miniaturized metamaterial CRLH bandpass filter structure has been proposed for the low band of the UWB system. The design methodology has been validated by the 3D EM simulations and measurement, and the comparison between the design and implementation shows agreement and excellent performance with the insertion of much less than < 1.8 dB, the return loss of less than -15 dB in the passband. Besides, as to the observation of the miniaturization, the BPF is as small as 26.5 mm × 26.7mm, and it is convincing that the proposed methodology works appropriately showing the miniaturization effect of over 60 %.

Acknowledgements

This work was supported by the Incheon National University Research Grant in 2014.

References

[1] S.-S. Lee, et al., "A WiX RF Transceiver for Gbps

- Wireless Communication,” *2011 IEEE International Conference on Consumer Electronics (ICCE 2011)*, Jan. 2011, pp. 427-428-64.
- [2] Y.-C. Chiou, Y.-F. Lee, J.-T. Kuo and C.-C. Chen, “Planar Multimode Resonator Bandpass Filters with Sharp Transition and Wide Stopband,” *IEEE International Microwave Symposium Digest*, 2008, 6, pp. 439-442.
- [3] A. Balalem, W. Menzel, J. Machac, and A. Omar, “A Simple Ultra-Wideband Suspended Stripline Bandpass Filter With Very Wide Stop-Band,” *IEEE Microwave and Wireless Components Letters*, 2008, 3, pp. 170-172.
- [4] R.C. Allison, “Compact edge coupled filter,” United States Patent 6762660 B2, July 2004.
- [5] C.-C. Yu, and K. Chang, “Novel compact elliptic-function narrowband bandpass filters using microstrip open-loop resonators with coupled and crossing lines,” *IEEE Trans. MTT*, 1998, 46, (7), pp. 952-958.
- [6] J. Zhang, J.-Z. Gu, B. Cui, and X.W. Sun, “Compact and harmonic suppression open-loop resonator bandpass filter with tri-section SIR,” *Prog. Electromagn. Res.*, 2007, PIER 69, pp. 93-100.
- [7] C. Caloz. and T. Itoh, “Electromagnetic metamaterials: transmission line theory and microwave application” (John Wiley & Sons, 2006).
- [8] Marques. R, Martin. F and Sorolla. M., “Metamaterials with negative parameters: theory, design, and microwaves applications” (John Wiley & Sons, 2008).
- [9] G. Jang and S. Kahng, “Design of a dual-band metamaterial bandpass filter using zeroth order resonance,” *Prog. Electromagn. Res. C*, 2010, 12, pp. 149-162.
- [10] J. Ju. and S. Kahng, “A compact UWB bandpass filter using a center-tapped composite right/left-handed transmission-line zeroth-order resonator,” *Microwave and Optical Technology Letters*, 2011, 9, pp. 1974-1976.
- [11] G. Jang and S. Kahng, “Design of a Metamaterial Bandpass Filter Using the ZOR of a Modified Circular Mushroom Structure,” *Microwave Journal*, 2011, 5, pp. 158-167.
- [12] H. Shaman and J. S. Hong, “Input and output cross-coupled wideband bandpass filter,” *IEEE Trans. Microw. Theory Tech.*, vol. 55, no. 12, pp. 2562-2568, Dec. 2007.
- [13] Hye-Min Lee, Jung-Hyun Ha, Xu-Guang Wang, Young-Ho Cho and Sang-Won Yun, “Microstrip Bandpass Filter Using Stepped-Impedance Coupled-Line Hairpin Resonators with Enhanced Stopband Performance,” *Journal of Electromagnetic Engineering And Science*, vol. 11, no. 2, pp. 91-96, 2011, 6.
- [14] V. M. Dabhi and V. V. Dwivedi, "Parallel coupled microstrip bandpass filter designed and modeled at 2 GHz," 2016 International Conference on Signal Processing, Communication, Power and Embedded System (SCOPEs), Paralakhemundi, 2016, pp. 461-466.
- [15] X.-G. Huang, Q.-Y. Feng, Q.-Y. Xiang and D.-H. Jia., “Design of Bandpass Filter with Transmission Zeros Using Zeroth-order Resonator and U-shaped Resonator,” *Progress In Electromagnetics Research Symposium Proceedings, Moscow, Russia, August 19-23, 2012*, 12, pp. 857-860.
- [16] J. Q. Gong and Q. X. Chu, “Miniaturized microstrip bandpass filter using coupled SCRLH zeroth-order resonators,” *2009 European Microwave Conference (EuMC), Rome, 2009*, pp. 370-373.
- [17] V. N. Mishra, R. K. Chaudhary, K. V. Srivastava and A. Biswas, “Compact two pole bandpass filter implemented using via-free composite right/left handed transmission line with radial stubs,” *2011 41st European Microwave Conference, Manchester, 2011*, pp. 571-574.
- [18] J. N. Lee, S. Kahng, G. Jang, J. K. Park, “Three-Channel Output Multiplexer Design Using Band-Pass Filter and Ultra-Wideband Antenna,” *Journal of Electromagnetic Engineering and Science*, vol. 17, no. 2, pp. 111-112, 2017



Changhyeong Lee He received B.E degree in Electronic Engineering from Incheon National University, Incheon, Korea, in 2016. He is currently working toward M. Eng. degree on radio science and engineering at the Department of Information and Telecommunication Engineering in Incheon National University. His research fields are microwave engineering, RF components and metamaterials.



Sungtek Kahng He received his Ph.D. degree in Electronics and Communication Engineering from Hanyang University, Korea in 2000, with a specialty in radio science and engineering. From 2000 to early 2004, he worked for the Electronics and Telecommunication Research Institute on numerical electromagnetic characterization and developed RF passive components for satellites. In March 2004, he joined the Department of Information and Telecommunication Engineering at Incheon National University where he has continued research on analysis and advanced design methods of microwave components and antennas, including metamaterial technologies, MIMO communication and wireless power transfer.